Classical diffusive dynamics for the quasiperiodic kicked rotor

Gabriel Lemarié, Dominique Delande, Jean Claude Garreau, Pascal Szriftgiser

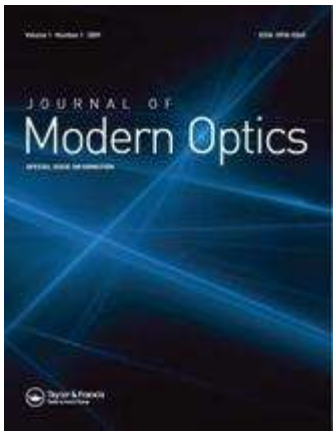

Classical diffusive dynamics for the quasiperiodic kicked rotor

Journal:	*Journal of Modern Optics*
Manuscript ID:	TMOP-2010-0111.R1
Manuscript Type:	Special Issue Paper - PQE 2010
Date Submitted by the Author:	n/a
Complete List of Authors:	Lemarié, Gabriel; CEA Delande, Dominique; CNRS Garreau, Jean Claude; CNRS Szriftgiser, Pascal; CNRS
Keywords:	Anderson Transition, Kicked rotor, Classical diffusion
Note: The following files were submitted by the author for peer review, but cannot be converted to PDF. You must view these files (e.g. movies) online.	
art-JMO-resub-2.tex	

Journal of Modern Optics
Vol. 00, No. 00, 00 Month 200x, 1–8

RESEARCH ARTICLE

Classical diffusive dynamics for the quasiperiodic kicked rotor

Gabriel Lemarié[a], Dominique Delande[b], Jean Claude Garreau[c] and Pascal Szriftgiser[c*]

[a]*Service de Physique de l'État Condensé (CNRS URA 2464), IRAMIS/SPEC, CEA Saclay, F-91191 Gif-sur-Yvette, France*;
[b]*Laboratoire Kastler Brossel, UPMC-Paris 6, ENS, CNRS; 4 Place Jussieu, F-75005 Paris, France*;
[c]*Laboratoire de Physique des Lasers, Atomes et Molécules, Université Lille 1 Sciences et Technologies, UMR CNRS 8523; CERLA; F-59655 Villeneuve d'Ascq Cedex, France*;
(*Received 00 Month 200x; final version received 00 Month 200x*)

We study the *classical* dynamics of a quasiperiodic kicked rotor, whose *quantum* counterpart is known to be an equivalent of the 3D Anderson model. Using this correspondence allowed for a recent experimental observation of the Anderson transition with atomic matter waves. In such a context, it is particularly important to assert the chaotic character of the classical dynamics of this system. We show here that it is a 3D anisotropic diffusion. Our simple analytical predictions for the associated diffusion tensor are found in good agreement with the results of numerical simulations.

1. Introduction

One of the most remarkable interference effects is certainly the Anderson localisation (*1*): A classical random walker displays diffusive dynamics. But a quantum-coherent one (i.e. which keeps a memory of its phase) can either diffuse, or localise. This depends on the relative importance of diffusive transport and interference effects.

Most studied wave systems which may show localisation are those where a wave propagates in a disordered medium, where disorder induces a random walk. However, the phenomenon of random walk is not restricted to disordered systems, as it can occur in very simple chaotic systems such as the well-known kicked rotor (*2*), described by the Hamiltonian:

$$H = \frac{p^2}{2} + K \cos x \sum_n \delta(t - n) \,, \tag{1}$$

where p is the momentum conjugated to the variable x (which, as it appears only in the argument of a cosinus, can be restricted to $[0, 2\pi]$), the particle mass is taken equal to unity and K represents the amplitude of the sinusoidal potential. This system has one degree of freedom, but the presence of a temporal forcing and its non-linear character allow the existence of a chaotic regime. More specifically, for values of the so-called stochasticity parameter $K \gtrsim 4$, the classical dynamics of that system along p is a random walk: the walker " particle p" diffuses (*2*).

In 1995, Raizen and coworkers realised a kicked rotor by exposing laser-cooled atoms to a pulsed standing wave (*3*), which is "seen" by the atoms as a sinusoidal potential acting on the centre of mass variables. However, for cold enough atoms, the de Broglie wavelength becomes comparable to the spatial period of the standing wave, in which case their dynamics is quantum

*Corresponding author. Email: Pascal.Szriftgiser@univ-lille1.fr

ISSN: 0950-0340 print/ISSN 1362-3044 online

DOI: 10.1080/0950034YYxxxxxxxx
http://www.informaworld.com

(wavelike) and one can observe the phenomenon of "dynamical localisation" (*3, 4*), that is, the freezing of the diffusive transport of the walker in the momentum space. This phenomenon has been shown to be equivalent to the Anderson localisation in 1D (*5–7*). An impressive surge of theoretical and experimental work on the subject followed (*8–20*).

The correspondence between the kicked-rotor and the Anderson model can be extended to higher dimensions: It turns out that a quasiperiodic kicked rotor with d incommensurable temporal frequencies is equivalent to a d dimensional Anderson model (*21–23*). Adding two new (incommensurate) frequencies to the Hamiltonian (1) thus prompts to the observation of the *Anderson transition*, which exists only in 3 (or higher) dimensions. We have engineered in our cold atom experiment (*24, 25*) a quasiperiodic realisation of the kicked rotor described by the Hamiltonian

$$H_{\rm qp} = \frac{p^2}{2} + K\cos x[1+\varepsilon\cos(\omega_2 t)\cos(\omega_3 t)]\sum_n \delta(t-n)\ . \tag{2}$$

to study and characterise this transition, including, in particular, the first non-ambiguous measurement of its critical exponent. Here, ε is the amplitude of the quasi-periodic modulation of the strength of the kicks, and the frequencies ω_2 and ω_3 must satisfy a condition of incommensurability.

It can be shown (*21, 25, 26*) that the above 1D system (2) has the same transport properties as that of the following 3D kicked "rotor":

$$H_3 = \frac{p_1^2}{2} + \omega_2 p_2 + \omega_3 p_3 + K\cos x_1[1+\varepsilon\cos x_2\cos x_3]\sum_n \delta(t-n)\ , \tag{3}$$

where $\boldsymbol{p} = (p_1, p_2, p_3)$ is the momentum conjugated to $\boldsymbol{x} = (x_1, x_2, x_3)$. In fact, the temporal evolution of an arbitrary initial condition $\psi_{\rm qp}(x, t=0)$ for $H_{\rm qp}$ (2) is identical to that of the corresponding ψ_3 :

$$\psi_3(\boldsymbol{x}, t=0) = \psi_{\rm qp}(x_1, t=0)\delta(x_2)\delta(x_3)\ , \tag{4}$$

for H_3 (3) (see (*25*)). Thus, our experience with the quasiperiodic kicked rotor can be regarded as an experience of transport of waves in a 3D medium originating from a time-pulse $\delta(t=0)$ of a plane source (invariant along the directions p_2 and p_3), where transport properties are actually observed in the direction perpendicular to the emitter. This presents strong similarities with the methods of study of transport of classical waves in 3D disordered media (*27*).

Note that (3) is not the standard 3D kicked rotor (*15*):

$$\tilde{H}_3 = \frac{p_1^2}{2} + \omega_2\frac{p_2^2}{2} + \omega_3\frac{p_3^2}{2} + K\cos x_1\cos x_2\cos x_3\sum_n \delta(t-n)\ . \tag{5}$$

Two characteristics of (3) are noteworthy: First, the linear dependence of the transverse kinetic energy in p_2 and p_3. Second, the "true" spatial direction "1" and the transverse "virtual" directions "2" and "3" present an anisotropy controlled by the parameter ε. How these features affect the classical dynamics of (3) as compared to that isotropically diffusive of (5) is the subject of this study.

Our motivations are the following. The linear dispersion of the transverse degrees of freedom in the Hamiltonian (3) seems, at first glance, to imply that only the direction "1" in (3) is disordered while the transverse directions "2" and "3" are quasiperiodic (see (*15, 25, 26, 28*)). This quasiperiodic character could prevent the classical transport in the transverse directions, thus making the localisation observed in the quantum regime not a consequence of subtle interference effects but attributable to the peculiar classical dynamics of this system (*29*). This is however

not the case. The classical dynamics of (3) is, as we shall see, fully diffusive in all directions, and the localisation observed in the quantum regime is therefore a quantum effect of the same nature as Anderson localisation. Second, the anisotropy of the classical transport is known to greatly affect the properties of the localisation, including a non-negligible dependence of the transition threshold on the degree of anisotropy (e.g. on the parameter ε) (*30*). We indeed observed such a dependence (see the phase diagram in (*25*)).

2. Analysis of the diffusive dynamics

The Hamiltonian (3) being periodic in time, its classical dynamics can be studied by adopting a stroboscopic point of view, e.g. by focusing on the system state just after the kicks. Integrating Hamilton's equations from a kick to the following one, we obtain the equivalent of the Standard Map (*2*) for this system, which relates values of the space and momentum vectors $(\boldsymbol{x}_n\ \boldsymbol{p}_n)$ just after the n_{th} kick to those $(\boldsymbol{x}_{n+1}, \boldsymbol{p}_{n+1})$ after a period:

$$\begin{aligned}
p_{1_{n+1}} &= p_{1_n} + K \sin\theta_{1_n}(1 + \varepsilon \cos x_{2_n} \cos x_{3_n}) \ , \\
p_{2_{n+1}} &= p_{2_n} + K\varepsilon \cos x_{1_n} \sin x_{2_n} \cos x_{3_n} \ , \\
p_{3_{n+1}} &= p_{3_n} + K\varepsilon \cos x_{1_n} \cos x_{2_n} \sin x_{3_n} \ , \\
x_{1_{n+1}} &= x_{1_n} + p_{1_{n+1}} \ , \\
x_{2_{n+1}} &= x_{2_n} + \omega_2 \ , \\
x_{3_{n+1}} &= x_{1_n} + \omega_3 \ .
\end{aligned} \tag{6}$$

Starting from an initial condition $(\boldsymbol{x}_0, \boldsymbol{p}_0)$, one can easily simulate the evolution of this system. In particular, we want to see how a state initially localised at $\boldsymbol{p}_0 = 0$ expands as time passes. Afterwards, only properties averaged over many initial conditions $\boldsymbol{p}_0 = 0$ and $\boldsymbol{x}_0 \in [0, 2\pi)$ will be considered.

Note that the temporal dependency (6) of the transverse variables x_2 and x_3 is trivial, and very different from that obtained from (5):

$$\begin{aligned}
x_{2_{n+1}} &= x_{2_n} + \omega_2 p_2 \ , \\
x_{3_{n+1}} &= x_{1_n} + \omega_3 p_3 \ .
\end{aligned} \tag{7}$$

However, from (6) we can express $p_{2_{n+1}}$ as:

$$p_{2_{n+1}} = p_{2_0} + K\varepsilon \sum_{j=1}^{n} \cos x_{1_j} \sin(x_{2_0} + \omega_2 j) \cos(x_{3_0} + \omega_3 j) \ , \tag{8}$$

which shows that the chaotic character of the motion in direction "1" progressively "diffuses" into the transverse directions, which hints for a complex dynamics in all directions. Indeed, as in the case of the 1D kicked rotor, the variables x_{1_j} can be considered as uncorrelated random variables, uniformly distributed over $[0, 2\pi)$ (the quasi-linear approximation is valid for large K) and p_2 thus also performs a random walk (*31*).

The randomisation of x_1 is due to two conjugated phenomena: the sensitivity on initial conditions and the folding of the phase-space. The sensitivity on initial conditions is characterised by the Kolmogorov-Sinaï entropy h (an average of individual Lyapounov exponents over a chaotic part or all of the phase space - see (*2*)), which gives the time-scale $1/h$ over which two trajectories initially close have diverged by $\delta x_1 \sim 2\pi$. The quasi-periodic action of x_2 and x_3 is to increase the entropy h, as compared to the standard case of the kicked rotor. Thus, we can say that the

variable x_1 is at least as random and uncorrelated as the variable x of the kicked rotor (*31*). Indeed, we know that, for $K \gtrsim 4$, the whole phase-space of the kicked rotor is chaotic and that x can be considered as an uncorrelated (or shortly correlated, the correlation time being $\sim 1/h$) variable. This will be true also for (6). However, for ε not too small, the threshold in K should be smaller. We have not dealt with this issue of the threshold of the diffusive transport in the 3D kicked "rotor" (3). In the following, we will restrict ourselves to values of K larger than 4.

The dynamics of the system in momentum space is thus diffusive, characterised by a diffusion tensor D_{ij} $(i, j = 1, 2, 3)$ defined as:

$$D_{ij} = \lim_{n\to\infty} \frac{\langle p_{i_n} p_{j_n}\rangle}{n} \tag{9}$$

where $\langle X\rangle$ represents the average of X over initial conditions. We can evaluate approximately this diffusion tensor. Let us consider the behaviour of $\langle {p_2}^2\rangle$, for example. We can write this quantity as:

$$\langle {p_2}_n{}^2\rangle = K^2\varepsilon^2 \sum_{j,m=1}^{n-1} \langle \cos x_{1_j} \cos x_{1_m}\rangle_{x_{1_0}} \times \langle \sin(x_{2_0} + \omega_2 j) \sin(x_{2_0} + \omega_2 m)\rangle_{x_{2_0}} \times$$
$$\times \langle \cos(x_{3_0} + \omega_3 j) \cos(x_{3_0} + \omega_3 m)\rangle_{x_{3_0}} . \tag{10}$$

The correlation function $\langle \cos x_{1_j} \cos x_{1_m}\rangle_{x_{1_0}}$ decreases exponentially in $|j - m|$, as in the case of the 1D kicked rotor (*31*). So the main contribution to the sum in (10) is given by $j = m$. Performing the average over the initial conditions, we finally obtain:

$$\langle {p_2}_n{}^2\rangle \approx \frac{K^2\varepsilon^2}{8} \times n , \tag{11}$$

in the quasi-linear approximation. Following those lines in the case of the other quantities $\langle p_i p_j\rangle$, we see easily that the diffusion tensor is diagonal and reads:

$$D_{11} \approx (K^2/2)(1 + \varepsilon^2/4) , \tag{12}$$
$$D_{22} \approx K^2\varepsilon^2/8 , \tag{13}$$
$$D_{33} \approx K^2\varepsilon^2/8 , \tag{14}$$
$$D_{i\neq j} \approx 0 . \tag{15}$$

From this, it is clear that the diffusive transport is anisotropic and that the axes "1", "2" and "3" are the principal axes. **Moreover, the system can be considered the chaotic equivalent of an anisotropic 3D Anderson model constituted of random chains coupled by the anisotropy strength ε, as considered in (*30*). Indeed, the case $\varepsilon = 0$ is realised via a collection of uncoupled chaotic chains, corresponding to $d = 1$, i.e. the usual 1D periodic kicked rotor (1).**

3. Confrontation with the results of numerical simulations

In this section we will compare the predictions of the previous sections with numerical simulations. First, we verify that the transport is indeed diffusive in all directions (for $K \gtrsim 4$), and that the non-diagonal coefficients $D_{i\neq j}$ of the diffusion tensor vanish. Figure 1 represents the temporal evolution of $\langle p_i p_j\rangle$ for the Hamiltonian (3) with $\omega_2 = 2\pi\sqrt{5}$ and $\omega_3 = 2\pi\sqrt{13}$ incommensurate with each other and with 2π (this condition of incommensurability corresponds to the case of the

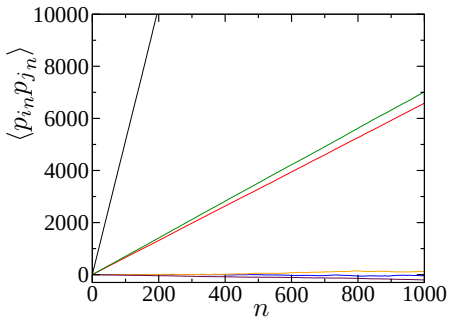

Figure 1. Time evolution of the correlation of classical momenta $\langle p_i p_j \rangle$. The non-diagonal terms $i \neq j$ (orange, blue and maroon) keep small values all along the evolution, whereas the diagonal terms increase linearly with time, the slope of $\langle {p_1}^2 \rangle$ (represented in black) being much larger than the slopes of $\langle {p_2}^2 \rangle$ (in red) and $\langle {p_3}^2 \rangle$ (in green). This shows that the dynamics is anisotropically diffusive and that "1", "2" and "3" are its principal axes. The dynamics is approximately the same along the axes "2" and "3" (see figure 5 (b)). The parameters are: $K = 10$, $\varepsilon = 0.8$, $\omega_2 = 2\pi\sqrt{5}$ and $\omega_3 = 2\pi\sqrt{13}$.

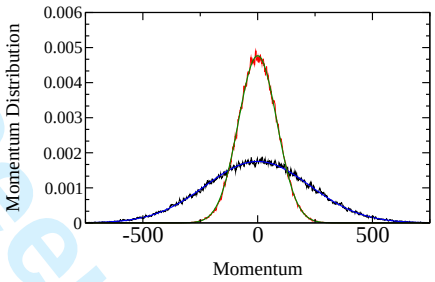

Figure 2. Final momentum distributions along p_1 (in black) and p_2 (in red), the distribution along p_3 being approximately identical to that along p_2. After 1000 kicks, they display all a Gaussian shape characteristic of a diffusive motion. The blue and green curves are fits by a Gaussian which do not show any statistically significant deviation. Parameters are $K = 10$, $\varepsilon = 0.8$, $\omega_2 = 2\pi\sqrt{5}$ and $\omega_3 = 2\pi\sqrt{13}$.

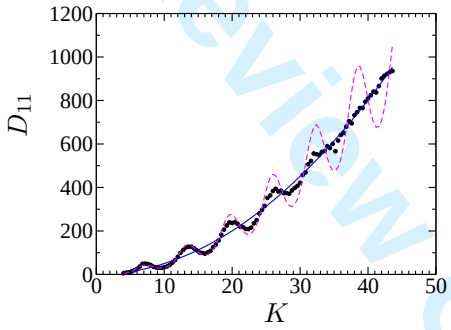

Figure 3. Dependence on K of the longitudinal diffusion coefficient D_{11} (black points) when the anisotropy is strong: $\varepsilon = 0.1$. One observes oscillations around the average behaviour equation (12) (represented in blue) which follow the known corrections of the kicked rotor, equation (16) (dashed magenta curve), but only for values of K not too large. When K is increased, these oscillations decrease faster than in the case of the kicked rotor. The parameters are the following: $\omega_2 = 2\pi\sqrt{5}$ and $\omega_3 = 2\pi\sqrt{13}$.

quasiperiodic kicked rotor), $K = 10$ and $\varepsilon = 0.8$. The time evolution of the diagonal terms $\langle {p_i}^2 \rangle$ is linear while the non-diagonal terms $\langle p_i p_{j \neq i} \rangle$ stay very close to zero. Also, the distribution of each p_i has a Gaussian shape, characteristic of a diffusive transport (see figure 2).

The dependence of the diffusion tensor versus K is now studied for $\varepsilon = 0.1$, when the anisotropy is strong, and for $\varepsilon = 0.8$, when the anisotropy is much weaker.

For $\varepsilon = 0.1$, $D_{11}(K)$ is found to oscillate around its average behaviour, equation (12), the amplitude of these oscillations decreasing as K increases. This recalls the oscillations of the diffusion coefficient of the 1D kicked rotor when K is varied. In the latter case, these oscillations appear due to the presence of residual correlations $\langle \sin x_n \sin x_0 \rangle$. Taking into account correlations

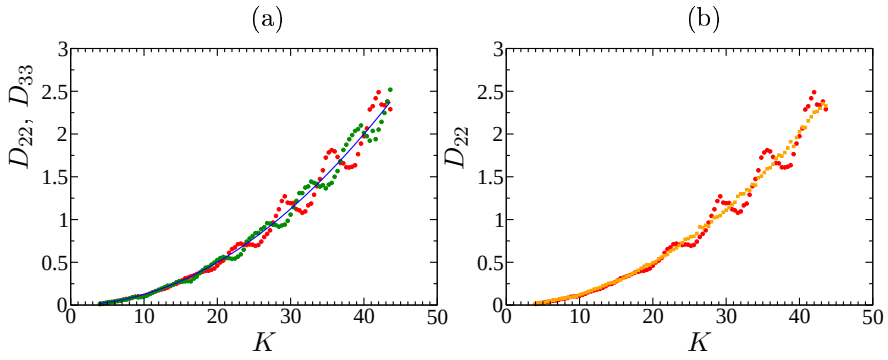

Figure 4. **(a) Dependence on K of the transverse diffusion coefficients D_{22} (red points) and D_{33} (green points) when the anisotropy is strong: $\varepsilon = 0.1$. The diffusion coefficients are found to oscillate around their average behaviour, equations (13) and (14). The oscillating corrections do not decrease in amplitude as K increases, and they have the same period of the oscillations of $D_{11}(K)$. (b) Comparison with the behaviour of D_{22} vs K for the Hamiltonian (5) where x_2 and x_3 follow equations (7) (orange points). In the latter case, no oscillating corrections are visible. The parameters are: $\varepsilon = 0.1$, $\omega_2 = 2\pi\sqrt{5}$ and $\omega_3 = 2\pi\sqrt{13}$.**

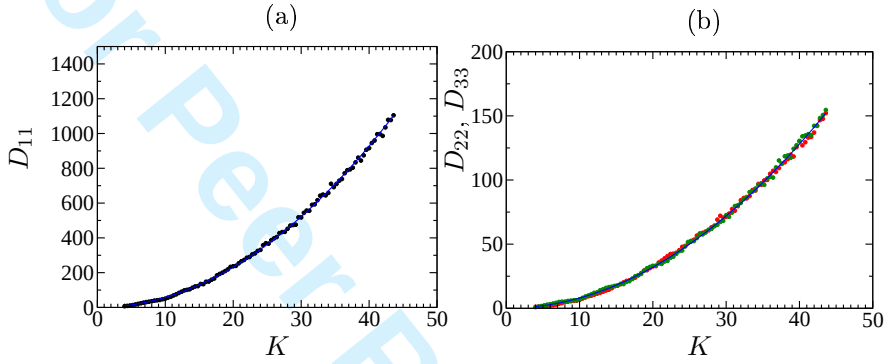

Figure 5. **Dependence on K of (a) D_{11} (black points), (b) D_{22} (red points) and D_{33} (green points) when the anisotropy is small: $\varepsilon = 0.8$. The diffusion coefficients closely follow the average behaviour predictions, equations (12), (13) and (14), represented in blue. In this case, correlations between kicks are all negligible. The parameters are: $\omega_2 = 2\pi\sqrt{5}$ and $\omega_3 = 2\pi\sqrt{13}$.**

up to four periods, it leads to the following approximation for the oscillations of $D(K)$ for the kicked rotor (*32*):

$$D(K) \approx \frac{K^2}{2}\{1 - 2J_2(K)[1 - J_2(K)]\} , \tag{16}$$

where $J_2(K)$ is the Bessel function of second order. In the case of the Hamiltonian (3), we expect a similar phenomenon to occur when ε is small. $D_{11}(K)$ should follow the same oscillations of $D(K)$ (16). This is indeed the case, but only for not too large values of K, as can be seen in figure 3. As K increases further, the oscillations of $D_{11}(K)$ are quickly killed and we recover the average behaviour equation (12).

The evolutions of the transverse diffusion coefficients D_{22} and D_{33} vs K for $\varepsilon = 0.1$ are represented in figure 4 (a). The oscillating corrections to the average behaviour equations (13) and (14) do not seem to decrease in amplitude. On the contrary, in the case of a true 3D anisotropic kicked rotor, **no oscillations are visible** (see figure 4 (b)). The trivial dependence of x_2 and x_3 in the case of the Hamiltonian (3) is certainly responsible for this.

When the anisotropy is weak, $\varepsilon = 0.8$, the residual correlations between kicks, responsible for the oscillating corrections on the diffusion tensor discussed above, are killed even for small K. This is clearly seen in figures 5 (a) and (b) where the diffusion tensor elements are found to closely follow their average behaviours, equations (12), (13) and (14).

In conclusion of this section, we have shown that the classical dynamics of the model Hamiltonian (3) truly corresponds to a 3D chaotic diffusion, anisotropic along the true spatial direction

"1" and the "virtual" directions "2" and "3". The comparison of numerical simulations with the calculations of sect. 2 shows a very good agreement.

4. Conclusion

In this paper, we have reported some important statistical properties of the classical transport in the 3D system corresponding to the quasiperiodic kicked rotor we have recently used to study the Anderson metal-insulator transition (*24, 25*). The classical dynamics has been shown to be fully diffusive in all directions, a prerequisite of the possibility of 3D Anderson localisation in the quantum regime. We have given a simple analysis of the anisotropic character of the transport, which is found to be in good agreement with numerical simulations. This should enable us to gain more insight into the metal-insulator phase diagram of the quasiperiodic kicked rotor (*33*).

References

(1) Anderson, P.W. Absence of Diffusion in Certain Random Lattices. *Phys. Rev.* **1958**, *109* (5), 1492–1505.
(2) Chirikov, B.V. A universal instability of many-dimensional oscillator systems. *Phys. Rep.* **1979**, *52* (5), 263–379.
(3) Moore, F.L.; Robinson, J.C.; Bharucha, C.F.; Sundaram, B.; et al. Atom optics realization of the quantum δ-kicked rotator. *Phys. Rev. Lett.* **1995**, *75* (25), 4598–4601.
(4) Casati, G.; Chirikov, B.V.; Ford, J.; et al. *Stochastic behavior of a quantum pendulum under periodic perturbation* ; Vol. 93, Springer-Verlag, Berlin, Germany, 1979; pp 334–352.
(5) Grempel, D.R.; Prange, R.E.; Fishman, S. Quantum dynamics of a nonintegrable system. *Phys. Rev. A* **1984**, *29*, 1639–1647.
(6) Altland, A.; Zirnbauer, M.R. Field Theory of the Quantum Kicked Rotor. *Phys. Rev. Lett.* **1996**, *77* (22) (Nov), 4536–4539.
(7) Altland, A. Diagrammatic approach to Anderson localization in the quantum kicked rotator. *Phys. Rev. Lett.* **1993**, *71* (1) (Jul), 69–72.
(8) Klappauf, B.G.; Oskay, W.H.; Steck, D.A.; et al. Observation of noise and dissipation effects on dynamical localization. *Phys. Rev. Lett.* **1998**, *81* (6), 1203–1206.
(9) Oberthaler, M.K.; Godun, R.M.; d'Arcy, M.B.; Summy, G.S.; et al. Observation of quantum accelerated modes. *Phys. Rev. Lett.* **1999**, *83* (22), 4447–4451.
(10) Deng, L.; Hagley, E.W.; Denschlag, J.; Simsarian, J.E.; Edwards, M.; Clark, C.W.; Helmerson, K.; Rolston, S.L.; et al. Temporal, Matter-Wave-Dispersion Talbot Effect. *Phys. Rev. Lett.* **1999**, *83* (26), 5407–5411.
(11) Jones, P.H.; Stocklin, M.M.; Hur, G.; et al. Atoms in Double-δ-Kicked Periodic Potentials: Chaos with Long-Range Correlations. *Phys. Rev. Lett.* **2004**, *93* (22), 223002.
(12) Jones, P.H.; Goonasekera, M.; Renzoni, F. Rectifying Fluctuations in an Optical Lattice. *Phys. Rev. Lett.* **2004**, *93* (7), 073904.
(13) Behinaein, G.; Ramareddy, V.; Ahmadi, P.; et al. Exploring the Phase Space of the Quantum delta-Kicked Accelerator. *Phys. Rev. Lett.* **2006**, *97* (24), 244101.
(14) Wang, J.; Gong, J. Proposal of a cold-atom realization of quantum maps with Hofstadter's butterfly spectrum. *Phys. Rev. A* **2008**, *77* (3), 031405(R)–31408.
(15) Wang, J.; García-García, A.M. Anderson transition in a three-dimensional kicked rotor. *Phys. Rev. E* **2009**, *79* (3), 036206.
(16) Ringot, J.; Szriftgiser, P.; Garreau, J.C.; et al. Experimental Evidence of Dynamical Localization and Delocalization in a Quasiperiodic Driven System. *Phys. Rev. Lett.* **2000**, *85* (13), 2741–2744.
(17) Szriftgiser, P.; Ringot, J.; Delande, D.; et al. Observation of Sub-Fourier Resonances in a Quantum-Chaotic System. *Phys. Rev. Lett.* **2002**, *89* (22), 224101.
(18) Lignier, H.; Chabé, J.; Delande, D.; Garreau, J.C.; et al. Reversible Destruction of Dynamical Localization. *Phys. Rev. Lett.* **2005**, *95* (23), 234101.
(19) Lignier, H.; Garreau, J.C.; Szriftgiser, P.; et al. Quantum diffusion in the quasiperiodic kicked rotor. *Europhys. Lett.* **2005**, *69* (3), 327–333.
(20) Chabé, J.; Lignier, H.; Cavalcante, H.; Delande, D.; Szriftgiser, P.; et al. Quantum Scaling Laws in the Onset of Dynamical Delocalization. *Phys. Rev. Lett.* **2006**, *97* (26), 264101.
(21) Casati, G.; Guarneri, I.; Shepelyansky, D.L. Anderson transition in a one-dimensional system with three incommensurable frequencies. *Phys. Rev. Lett.* **1989**, *62* (4), 345–348.
(22) Basko, D.M.; Skvortsov, M.A.; Kravtsov, V.E. Dynamic Localization in Quantum Dots: Analytical Theory. *Phys. Rev. Lett.* **2003**, *90* (9) (Mar), 096801.
(23) Lemarié, G.; Grémaud, B.; Delande, D. Universality of the Anderson transition with the quasiperiodic kicked rotor. *Europhys. Lett.* **2009**, *87*, 37007.
(24) Chabé, J.; Lemarié, G.; Grémaud, B.; Delande, D.; Szriftgiser, P.; et al. Experimental Observation of the Anderson Metal-Insulator Transition with Atomic Matter Waves. *Phys. Rev. Lett.* **2008**, *101* (25), 255702.
(25) Lemarié, G.; Chabé, J.; Szriftgiser, P.; Garreau, J.C.; Grémaud, B.; et al. Observation of the Anderson metal-insulator transition with atomic matter waves: Theory and experiment. *Phys. Rev. A* **2009**, *80* (4), 043626.
(26) Shepelyansky, D.L. Localization of diffusive excitation in multi-level systems. *Physica D* **1987**, *28*, 103–114.
(27) Störzer, M.; Gross, P.; Aegerter, C.M.; et al. Observation of the Critical Regime Near Anderson Localization of Light. *Phys. Rev. Lett.* **2006**, *96* (6), 063904.

(28) Fishman, S.; Grempel, D.R.; Prange, R.E. Chaos, quantum recurrences, and Anderson localization. *Phys. Rev. Lett.* **1982**, *49*, 509–512.
(29) Albert, M.; Leboeuf, P. Localization by bichromatic potentials versus Anderson localization. *Phys. Rev. A* **2010**, *81* (1), 013614–Phys.Rev.A81,013614(2010)[8pages].
(30) Panagiotides, N.A.; Evangelou, S.N.; Theodorou, G. Localization-delocalization transition in anisotropic solids. *Phys. Rev. B* **1994**, *49* (20), 14122–14127.
(31) Shepelyansky, D.L. Some statistical properties of simple classically stochastic quantum systems. *Physica D* **1983**, *8*, 208–222.
(32) Rechester, A.B.; Rosenbluth, M.N.; White, R.B. Fourier-space paths applied to the calculation of diffusion for the Chirikov-Taylor model. *Phys. Rev. A* **1981**, *23* (5), 2664–2672.
(33) Lemarié, G.; Delande, D. *in preparation* **2010**.

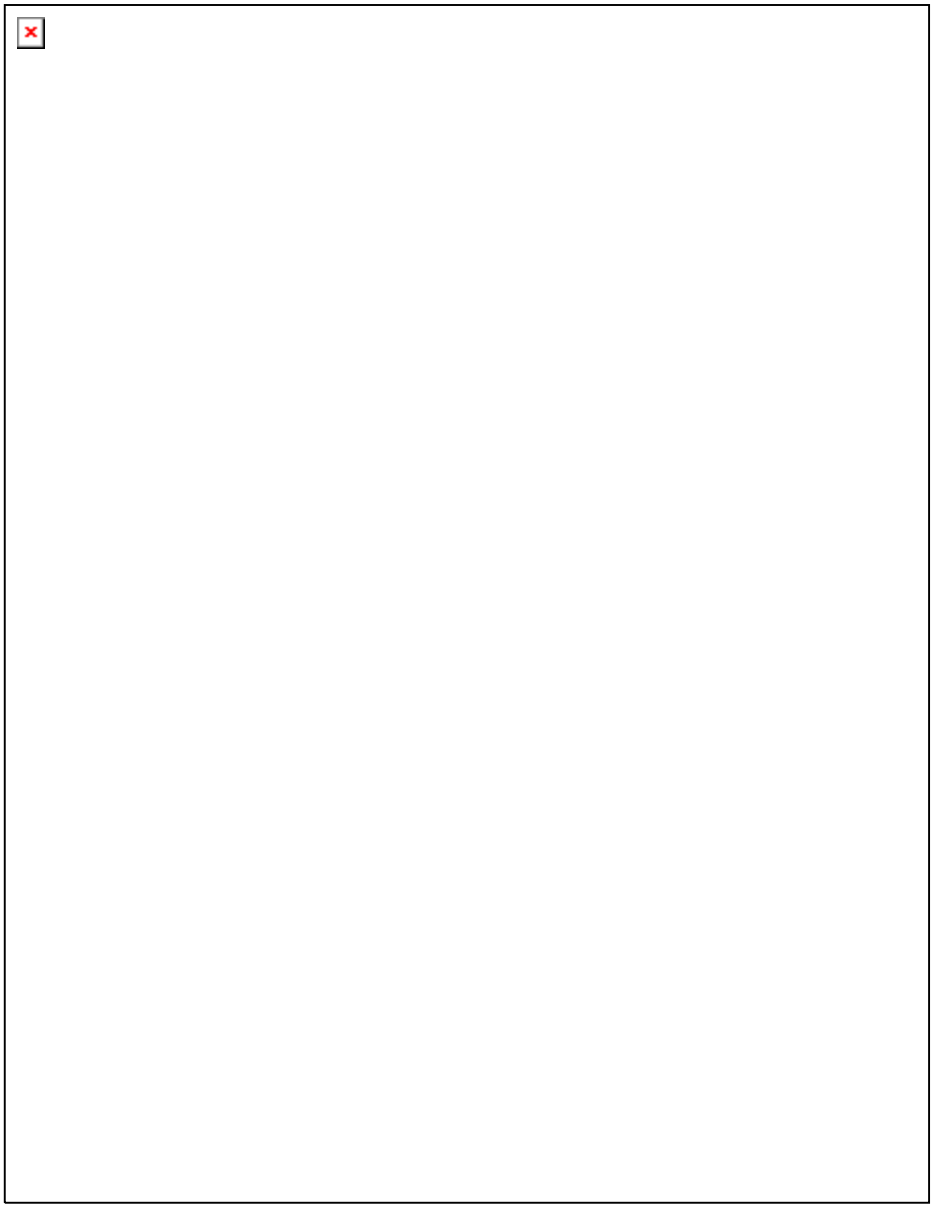

215x279mm (600 x 600 DPI)

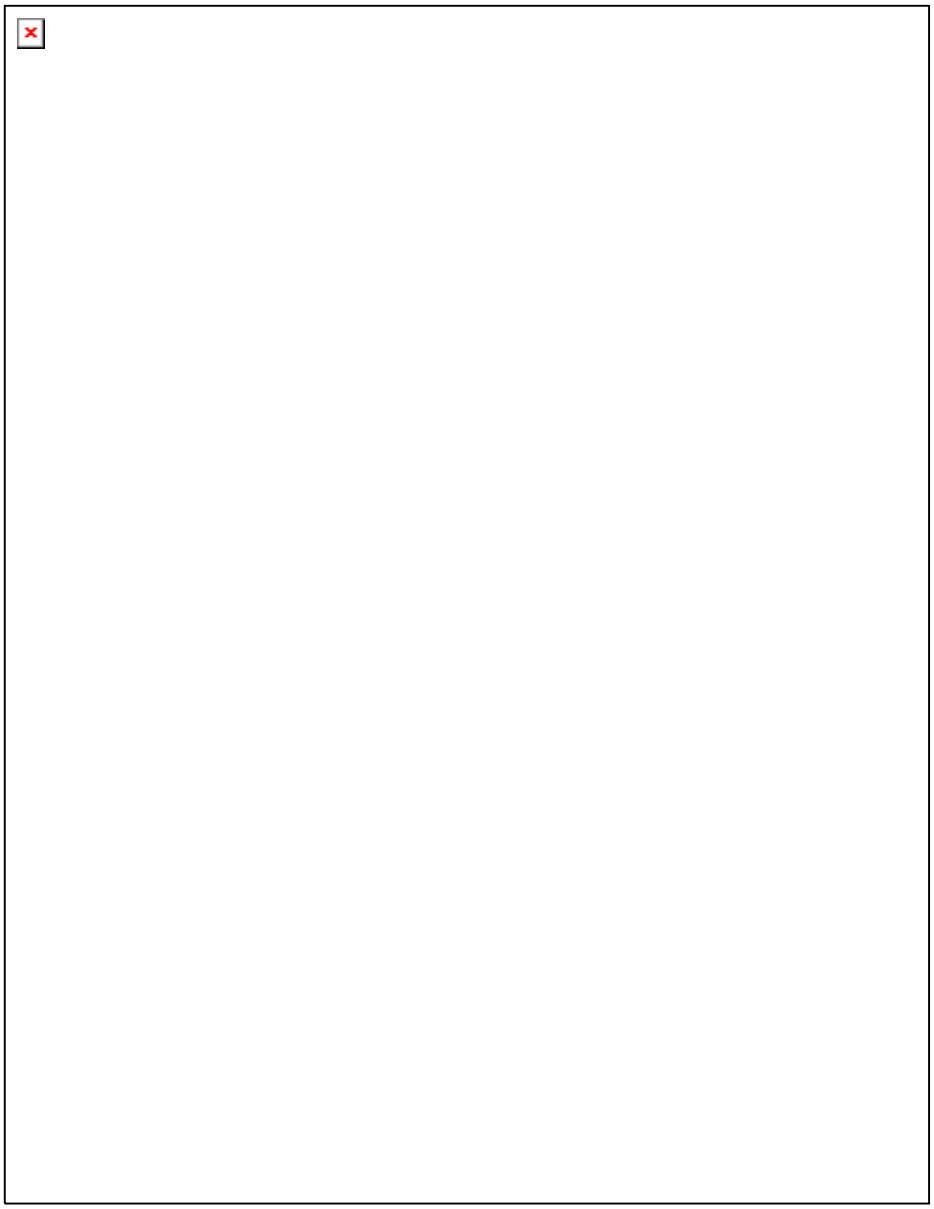

215x279mm (600 x 600 DPI)

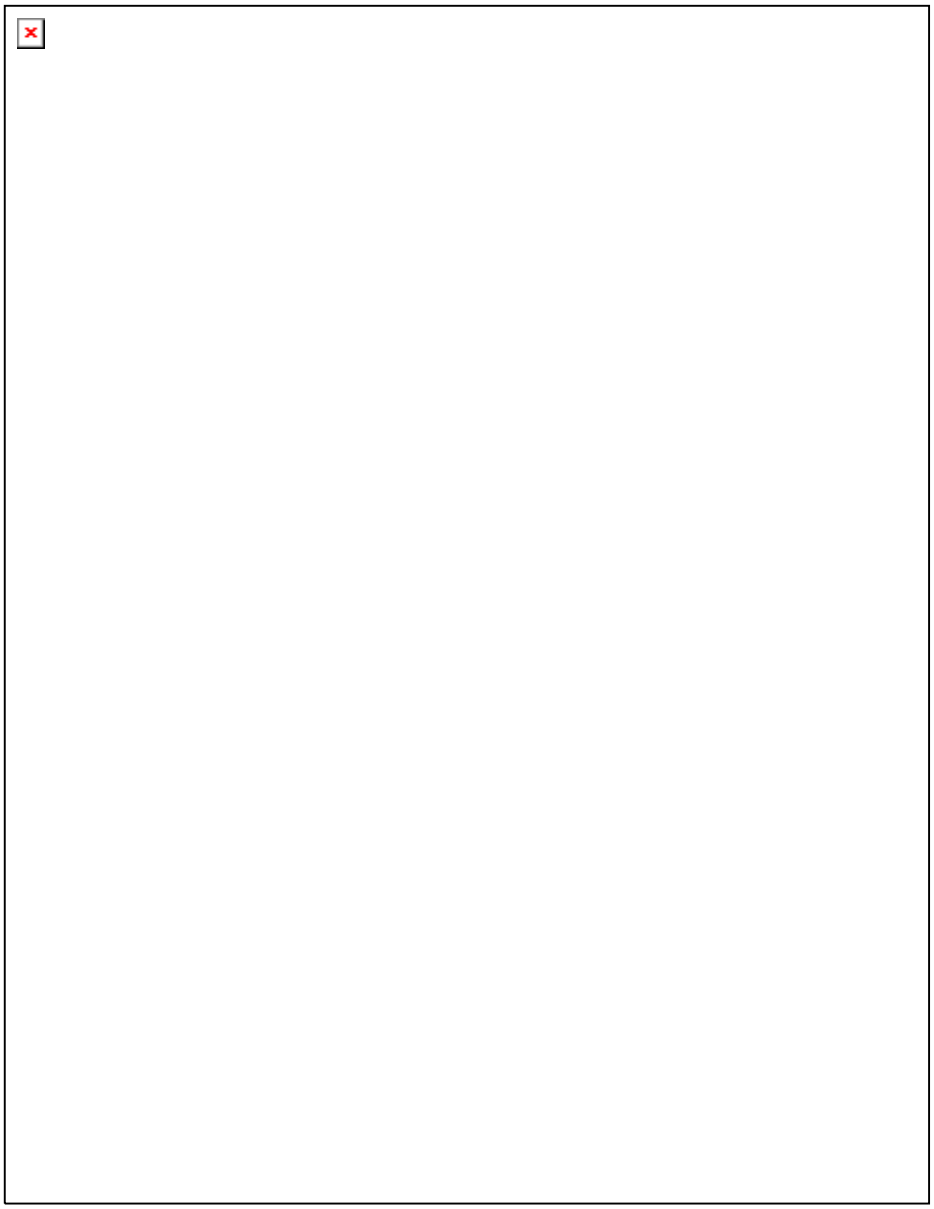

215x279mm (600 x 600 DPI)

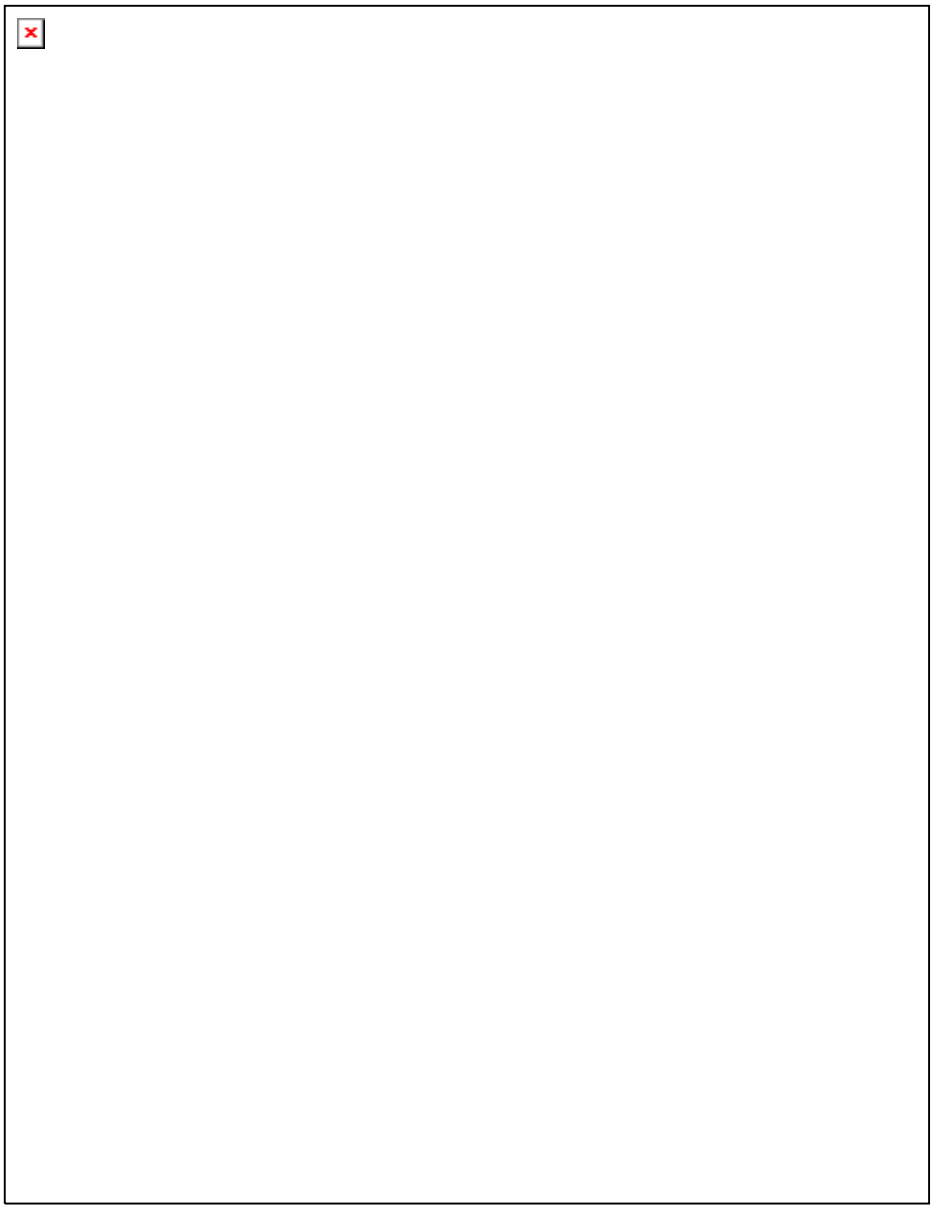

215x279mm (600 x 600 DPI)

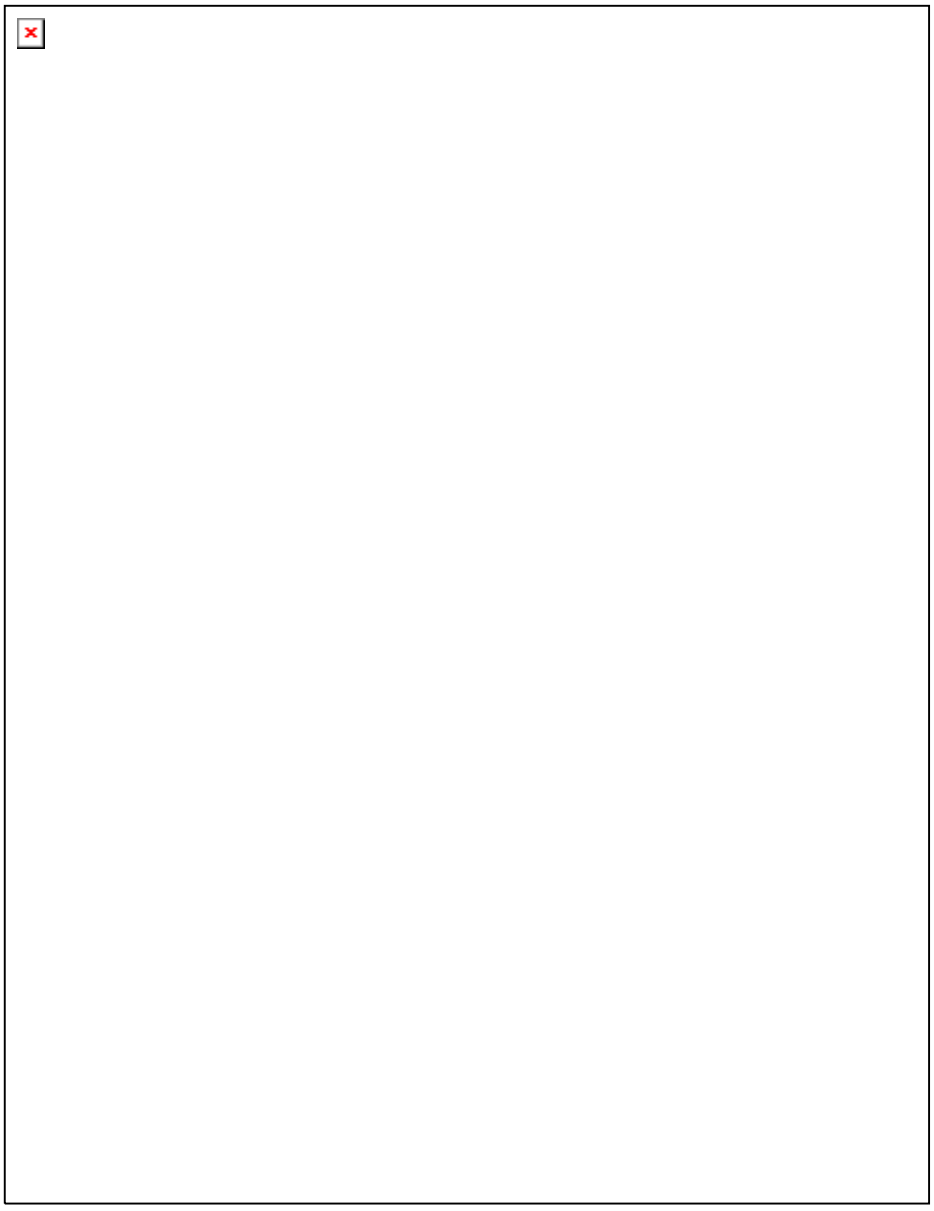

215x279mm (600 x 600 DPI)

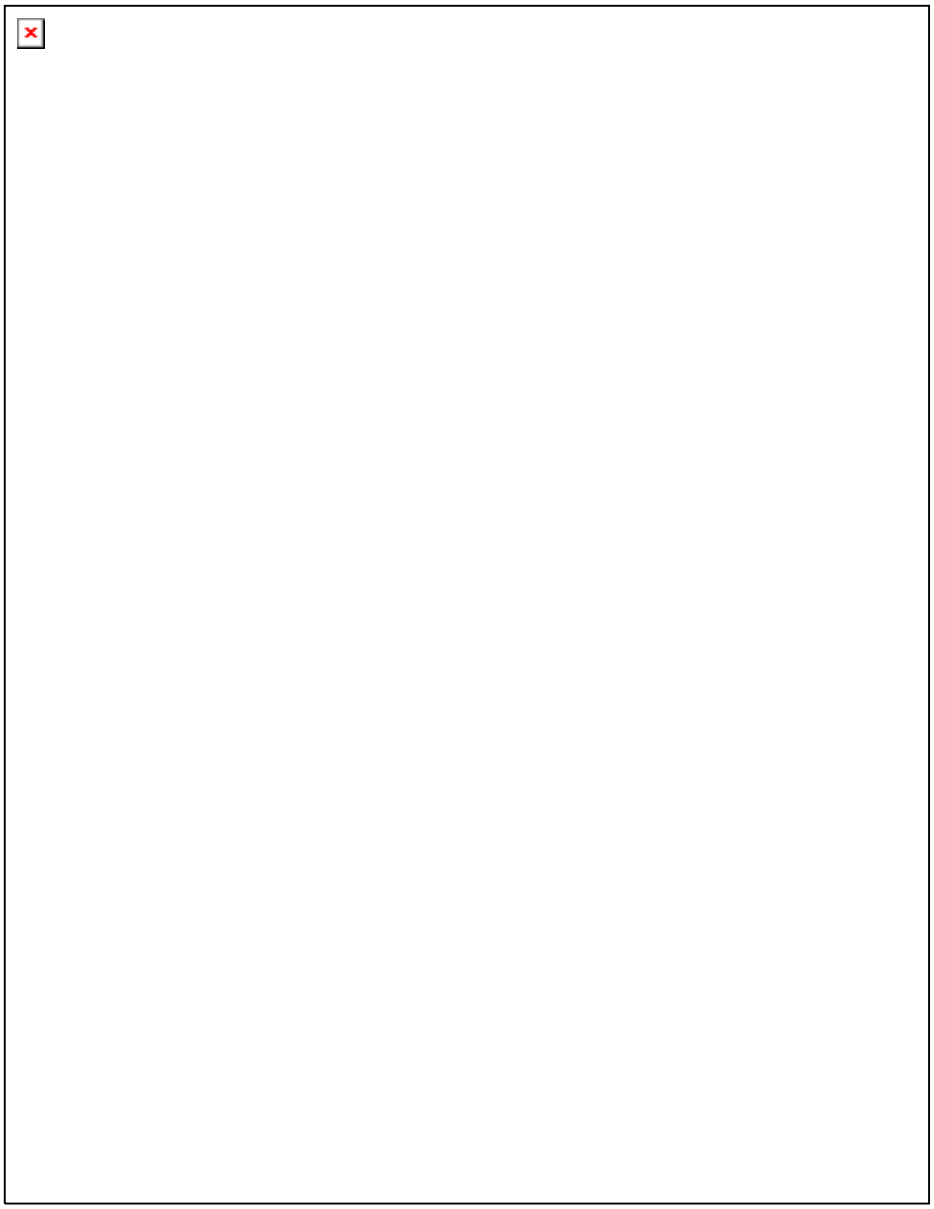

215x279mm (600 x 600 DPI)

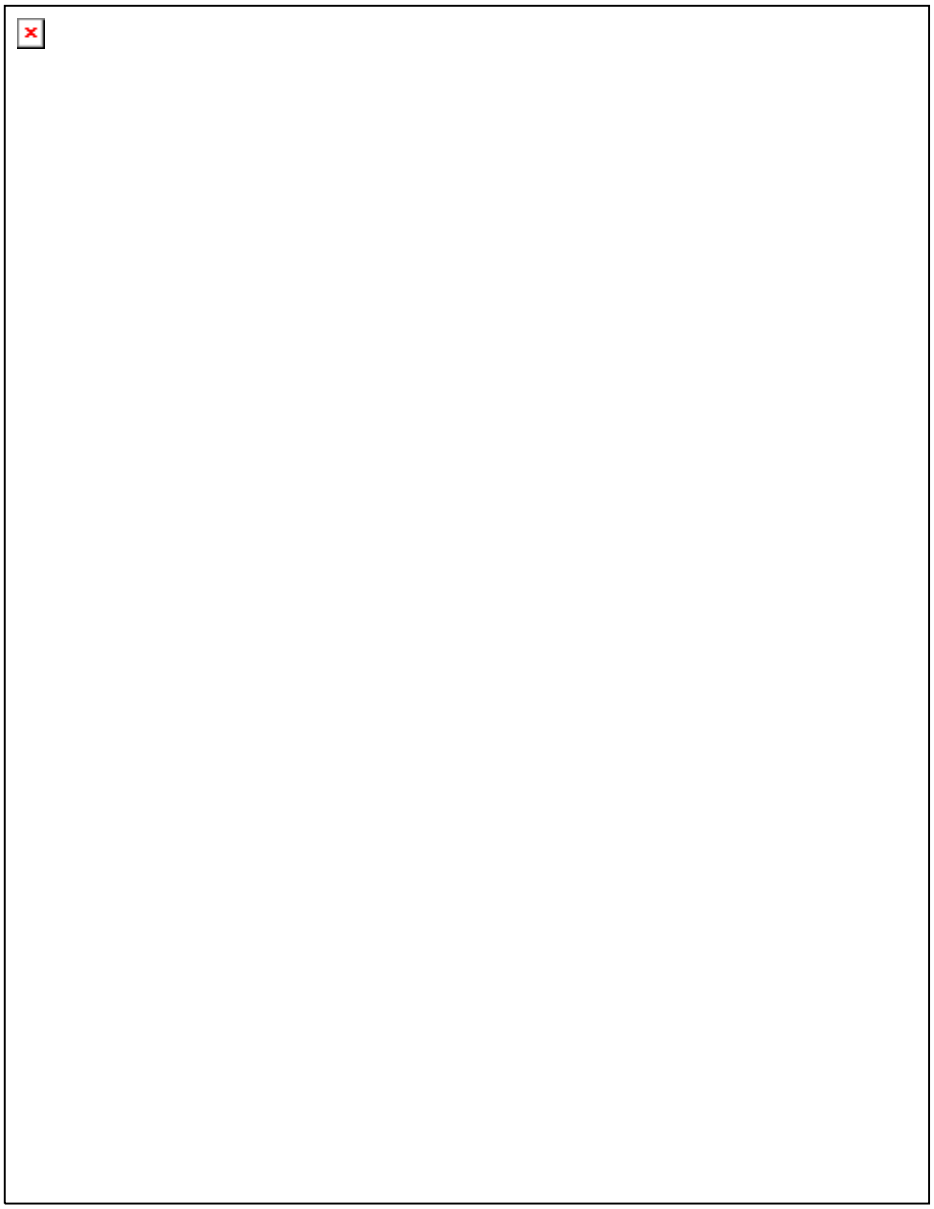

215x279mm (600 x 600 DPI)